

Review

An Overview of Fabricating Nanostructured Electrode Materials for Biosensor Applications

Rasu Ramachandran¹, Shen-Ming Chen^{2,*}, George peter Gnana kumar³, Pandi Gajendran¹,
Natrajan Biruntha Devi⁴,

¹The Madura College, Department of Chemistry, Vidya Nagar, Madurai – 625 011, Tamil Nadu, India.

²Electroanalysis and Bioelectrochemistry Lab, Department of Chemical Engineering and Biotechnology, National Taipei University of Technology, No.1, Section 3, Chung-Hsiao East Road, Taipei 106, Taiwan (ROC).

³Department of Physical Chemistry, School of Chemistry, Madurai Kamaraj University, Madurai-625 021, Tamil Nadu, India.

⁴Department of Chemistry, S.Vellaichamy Nadar College, Nagamalai pudukkottai, Madurai – 625021, Tamil Nadu, India.

*E-mail: smchen78@ms15.hinet.net

Received: 17 May 2015 / *Accepted:* 13 August 2015 / *Published:* 26 August 2015

Over past few decades different types of nanostructured electrode materials have been reported for the electrochemical analysis and biosensor applications. This article will give overview on the electrode materials based on carbon fiber, carbon nanotube (Single-walled carbon nanotubes and multi-walled carbon nanotubes), graphene oxide, metal oxide, conducting polymer and nanocomposites. The different electrochemical methods such as cyclic voltammetry, square wave voltammetry, differential pulse voltammetry, amperometry, electrochemical impedance spectroscopy and analytical methods such as UV-visible spectroscopy have also been overviewed. The biosensing applications of these nanostructured electrodes to the determination of biologically important analytes such as glucose, cholesterol, dopamine, uric acid, ascorbic acid, chitosan, cytochrome c, paraxon, acetylcholinesterase and hypoxanthine have also been reviewed. There are good prospects to fabricate low cost electrode materials, new conception and attractive aspect for the development of future biosensor applications.

Keywords: Nanostructured materials, Electroanalytical methods, Electrochemistry, Biosensor, Enzyme electrodes.

1. INTRODUCTION

The electrochemical biosensors are attractive methods for the sensitive determination of analytes in terms of low sensitivity, selectivity and long term stability [1]. Several reviews on specific

application of different modified electrode materials used in biosensors [2-9] and energy storage [10, 11] device are available in reported literature. Nanocomposite modified electrodes display fascinating electrochemical properties in pesticide sensor [12] and non-enzymatic sensor [13] applications. The discovery of two-dimensional graphene based electrode material has been used for direct electron transfer from cytochrome C and reduction of nitric oxide [14]. The highly ordered mesoporous carbon-fullerene based modified electrode facilitated direct quantifications of β -nicotinamide adinine dinucleotide (NADH), ascorbic acid (AA), uric acid (UA), dopamine (DA) and epinphrine (EP) [15]. A novel polyvinylpyrrolidone protected graphene/polyethylenimine-functionalized/ionic liquid/glucose oxidase electrode has shown excellent biocompatibility with glucose biosensors [16]. Much electrochemical biosensor detection has been demonstrated on graphene based modified electrodes, i.e., graphene-chitosan/haemoglobin/graphene/ionic liquid [17]. Among the graphene based materials, chemically reduced graphene oxide modified glassy carbon (CR-GO/GC) electrode has significantly improved catalytic performance in biosensors [18]. The immobilized acetylcholinesterase based carboxyphenylboronic/reduced graphene oxide-gold nanocomposite enhanced the electrochemical sensitivity of biomolecular reaction and presents rapid response with low detection limit [19]. Graphene oxide and sheet-mediated silver composite exhibit excellent electrochemical biosensing ability and sensitively detects the pathogenic bacteria, protein and DNA [20]. Water-soluble polyhydroxylated fullerene derivatives have been extensively exploited for haemoglobin biosensor and to improve the anti-oxidant properties [21]. The most described immobilized acetylcholinesterase on a novel TiO₂-decorated graphene nanohybrid can be monitored by measuring a good performance of organophosphate pesticide sensor analysis [22]. On the other hand, a disposable biosensor based on tyrosinase-protected gold nanoparticle (Tyr-Au) was immobilized with 1-pyrenebutanoic acid, succinimidyl ester and graphene oxide (PASE-GO) forming a biocompatible nanocomposite and it was coated with screen-printed electrode (SPE) for the determination of phenolic compounds [23]. Electrochemical DNA sensor has been evaluated by carboxyl functionalized graphene oxide and it was electropolymerized with poly-L-lysine on glassy carbon electrode. The polymerized composite (GO-COOH/PLLY/GCE) immobilized with ssDNA for the detection of vibrio parahemolyticus (*tlh* gene) [24]. The human live cell secretion of H₂O₂ has been detected by ultrasonic-electrodeposited of triple component designed with Pt-MnO₂/graphene nanohybrid electrode [25]. Graphene oxide and nafion based electrode with incorporated with myoglobin (Mb-GO-nafion) have also been exploited as electrode in biosensors. In this Mb film electrode exhibited good electrocatalytic activities towards H₂O₂, nitrite and oxygen [26].

The outline of this article overviewed various nanostructured electrode materials, different electrochemical techniques and promising electrochemical application for the detection of biosensing molecules. Finally, special interest highly focused on effect of morphological structure, optimized pH, low limit of detection, high sensitivity and long term durability in electrochemical biosensors application.

2. ELECTRODE MATERIALS FOR BIOSENSORS

2.1. Carbon fiber

Carbon fiber electrode materials are readily available and it act multi-properties like high electrochemical stability, low electrical resistivity and high mechanical strength. The carbon fibre electrode modified with poly β -aminoanthraquinone (pAAQ) for the study of amperometric micro sensor of haemoglobin (HB) [27]. Voltammetric technique can be used for the optimization of electrochemical stability of modified electrode. Biosensing molecule of HB, the amperometric response range of 0.5 μM to 340 μM and the average current response value of about 23.2 nA. Carbon fiber electrode can be modified with co-deposition of ruthenium (Ru) and rhodium (Rh) nanoparticles. The modified electrode has been immobilized with glutamate dehydrogenase (GLUD) and it can be analyzed for the evaluation of α -ketoglutarate (α -KG) [28]. The amperometric response current range between 100 to 600 μM and the lowest limit of detection (LOD) value is 20 μM . The unmodified electrode of tyrosinase based carbon fiber paper suggests the monitoring of phenolic compounds like catechol, phenol, bisphenol and 3-aminophenol. The LOD value of catechol (2 nM), phenol (5 nM), bisphenol (5 nM) and 3-aminophenol (12 nM) [29]. A stable carbon fibre electrode modified during the co-immobilisation of acetylcholinesterase (AChE) and choline oxidase (ChOx) in bovin serum albumin (BSA) membrane for the development of acetylcholine and choline. A conventional three electrode optimized potential value of 800 – 1100 mV vs Ag/AgCl, exhibited LOD value of 1 μM for acetylcholine and choline. The biosensor exhibited good sensitivity and selectivity for acetylcholine and choline [30]. Deng *et al* [31] used a silk derived carbon fibre modified with Au@Pt urchinlike nanoparticles (Au@Pt NPs) for the development of Escherichia coli (E-Coli)-based electrochemical sensor. The reported LOD value of 0.09 mg L⁻¹ and it possesses high conductivity, high electrocatalytic activity and biocompatibility.

2.2. Carbon nanotube

Single-walled carbon nanotube (SWCNT) immobilized with 11-(ferrocenyl)-undecyltrimethyl ammonium bromide (FTMA) has been employed for the direct electron transfer of glucose oxidase (GOx) [32]. The voltammetric results are clearly indicated that the direct electron transfer between immobilized of GOx and surface of the modified SWCNT electrode. The measured glucose concentration against a linear relationship steady-state current has been estimated over a range from 0.04 – 0.38 mM. The immobilized modified electrode exhibited high sensitivity and good chemical stability. The acid treated carbon nanotube was immobilized with acetylcholinesterase (AChE) and the electronegative charged CNT surface was modified with a cationic poly(dimethylammonium chloride) (PDDA) layer [33]. A highly sensitive amperometric biosensor of PDDA/AChE/PDDA/CNT/GCE unique sandwich-like composite electrode for organophosphate pesticide analysis, the optimized sensors parameters like inhibition time regeneration conditions and LOD value of (0.4 pM) D-amino acid oxidase oncarboxylated multi-walled carbon nanotube/copper nanoparticle/polyaniline hybrid film have been fabricated on gold electrode, the immobilized composite for D-alanine from fruit juice

[34]. In this sensor study, a linear relationship between biosensor and D-alanine concentration range from 0.001 to 0.7 mM, the LOD of 0.2 mM and the sensitivity of $54.85 \text{ mA cm}^{-2} \text{ mM}^{-1}$. Apetric *et al* [35] have used carboxyl functionalized single-walled carbon nanotube electrode immobilized with Tyrosinase to employ an amperometric biosensing analysis of tyramine. This modified CNT electrode is suitable for environment for the study of bioactivity of tyrosinase. This bioactive reaction has a good linearity with the concentration of tyramine in the range from 5 – 180 μM and exhibited limit of detection of 0.62 μM .

2.3. Fullerene

A fullerene- C_{60} /glassy carbon electrode (FLR/GCE) have used for the interactions study of carbidopa (CD) with double standard calf thymus DNA (dsDNA) by using phosphate buffer solution (pH = 4.0) [36]. Cyclic voltammetry (CV), linear sweep voltammetry (LSV) and square wave voltammetry (SWV) techniques have used in the interaction study of CD with dsDNA. Similarly, UV-visible and fluorescence spectroscopy have monitored the interaction between CD and dsDNA. Apply SWV in a linear response of dsDNA concentration range between 0.1 to 25 nM and the reported LOD value of 0.03 nM, however the fabricated electrode expressed good repeatability, reproducibility and long term stability. A tentative application of fullerene and gold nanoparticle have examined for the development of nanostructured enzyme based biosensor and evaluation of polyphenol [37]. Surface Plasmon resonance spectroscopy (SPR), CV and chronoamperometry have been used for the characterization of modified electrode surface area and their biocatalytic activity. The biosensor showed fast amperometric response to gallic acid and a standard for poly phenol analysis of wine, the amperometry linear range from 0.03 – 0.30 m mol L^{-1} and the reported LOD value of 1.1 mg L^{-1} . Sheng *et al* [38] used a haemoglobin (Hb) immobilized fullerene-nitrogen doped carbon nanotube and chitosan (C_{60} -NCNT/CHIST) composite for sensing H_2O_2 . The composite showed a well defined redox peak values of $E_0 = -335 \text{ mV vs SCE}$ and assigned the redox reaction of Hb ($\text{Fe}^{\text{III}}/\text{Fe}^{\text{II}}$). The immobilized Hb have been optimized the fast electron transfer rate order processes of $k_s = 1.8 \text{ s}^{-1}$, the LOD value of 1 μM and the sensitivity of 438 mA mM^{-1} . An air-plasma activated fullerene impregnated to screen printed electrode was immobilized with DNA for the detection of Escherichia coli 16S rDNA [39]. The fullerene modified lipid bilayer membrane (s-BLMS) electrode have been used an electrochemical sensor for the detection of neutral odorant molecules [40], by using voltmmetry analysis, the two systems (I_2/I^- and ferrocene/ferrocinium) were studied with C_{60} lipid bilayer modified electrode. The results are clearly indicated that, C_{60} I_2/I^- exhibit more sensitivity than C_{60} ferrocene/ferrocinium.

2.4. Graphene oxide

Electrochemically reduced graphene oxide modified with multi-walled carbon nanotube (ERGO-MWCNT) on glassy carbon electrode for the detection of glucose [41]. The modified composite electrode exhibited high electrocatalytic activity of glucose oxidation and the LOD of 4.7

μM , the real sample of glucose obtained from human blood serum. Electrodeposition of hybrid film composed with laccase, tyrosinase, gold nanoparticles and chitosan on graphene doped carbon paste (LACC-TYR-AuNPs-CS/GPE) electrode used for the development of carbamate pesticide sensor collected from citrus fruits [42]. In this (LACC-TYR-AuNPs-CS/GPE) composite have used for the evaluation of Michaelis-Menten kinetic constant (k_m) value ($26.9 \pm 0.5 \text{ M}$). A titania nanosheet modified reduced graphene oxide ($\text{TiO}_2\text{NS-rGO}$) composite was immobilized with haemoglobin and it can be used for electrochemical analysis of H_2O_2 and nitrite [43]. The morphological and structural analysis has been characterized by SEM, XRD and Raman spectroscopy. The immobilized $\text{TiO}_2\text{NS-rGO}$ electrode displayed good electrochemical biosensor performance for the detection of H_2O_2 and nitrite, i.e. a wide linear range of $0.1 - 145 \mu\text{M}$ for H_2O_2 and $1 - 15,000 \mu\text{M}$ for nitrite, the LOD of 10 nM for H_2O_2 and $0.21 \mu\text{M}$ for nitrite. Peng *et al* [44] have used gold nanoparticle/toluidine blue-graphene oxide (AuNPs/TB-GO) composite, a facile and sensitive labile-free electrochemical DNA biosensor of multidrug resistance (MDR) gene. The sensor part has been analyzed by two different electrochemical techniques, such as electrochemical impedance spectroscopy (EIS) and differential pulse voltammetry (DPV), by employing the DPV hybridization of DNA measured from the peak current of TB. The currents were proportional to the logarithmic of the concentration of DNA, the optimized range from $1.0 \times 10^{-11} - 1.0 \times 10^{-9} \text{ M}$ and the LOD of $2.95 \times 10^{-12} \text{ M}$. A new type of electrochemical biosensor has been analyzed by used human serum albumin/graphene oxide/3-amino propyl triethoxy silane modified with indium tin oxide (ITO/APTES/GO/HSA) electrode used for the determination of enantiomers D and L – tryptophan (Trp) [45]. The composite electrodes were investigated by CV method, the exhibited oxidation peak potential of D and L trp occur at 860 and 1260 mV vs SCE respectively.

2.5. Metal oxides

Recently, metal oxides can offer promising electro active materials due to enhancement of the electrochemical reversible redox reaction, wide potential window and large surface-volume ratio. A nanostructure of metal oxide (CeO_2)-chitosan (CH) made electrode used as biosensor for sensing cholesterol molecule [46]. The fabricated ITO- CeO_2 -CH nanocomposite immobilized with cholesterol oxidase (ChOx). A novel core-shell zinc oxide based (ZnO /chitosan-graft-poly(vinyl alcohol)) (ZnO /CHIT-g-PVAL) nanocomposite led to the sensing of glucose, the composite reported LOD value of $0.2 \mu\text{M}$ [47]. Nanoparticle of titanium oxide modified with reduced graphene oxide (TiO_2 /NPs-rGO) composite has been immobilized to haemoglobin (Hb) for a mediator-free biosensor of hydrogen peroxide (H_2O_2), the LOD value of 10 nM [48]. Glucose biosensor for millimolar level determination of glucose generated with a glucose oxidase immobilized with cellulose tin-oxide (SnO_2) hybrid nanocomposite electrode [49]. A three layer of magnetic core-shell Au- Fe_3O_4 @ SiO_2 metal oxide based nanocomposite electrode used as a novel electrode materials for the detection of bioenzyme glucose biosensor applications [50]. Jeyaprakasam *et al* [51] have recently reported that acetylcholinesterase (AChE) enzyme immobilized with iron oxide-chitosan nanocomposite film modified glassy carbon

electrode (AChE/Fe₃O₄-CH/GCE) electrode can served as an excellent biosensor detection value of 3.6×10^{-9} M.

2.6. Conducting polymers

Conducting polymers (polythiophene, polyaniline and polypyrrole) have considerable application in optical, electrical and electrochemical properties. A number of authors have reviewed for the preparation, properties and applications of conducting polymers [52-54]. Electrodeposition of conducting polymers of poly(4,7-di(2,3)-dihydrothienol) [3,4-b] [1,4] dioxin-5-yl-benzo[1,2,5] thiazole (PBDT) and poly(4,7-di(2,3)dihydrothienol[3,4-b] [1,4] dioxin-5-yl-2,1,3-benzoselenadiazole (PESeE) on graphite electrode, the modified electrodes were immobilized with glucose oxidase (GO) and the biosensor's LOD value of 0.05 mM for PBDT and 0.01 mM for PESeE [55]. Gokoglan *et al* [56] have electrochemically deposited a conducting polymer of poly(4,7-bis(thieno[3,2-b] thiophene-2-yl) benzo[c] [1,2,5] selenadiazole) poly(BSeTT) on gold electrode. The immobilized conducting polymers which can be apply for the biosensor detection of pyranose, the LOD value is 0.229 mM. There has been explosive growth of conducting polymer poly(4-(2,5-di(thiophene-2-yl)-1H-pyrrole-1-yl)-benzenamine) (poly(SNS-NH₂)) on graphite electrode for acetylcholine biosensor. The electrode leads to the LOD value of 0.11 mM [57]. The attractiveness of conducting polymers of 2-Heptyl-4,7-di(thiophene-2-yl)-1H-benzo[d] imidazole) (BImTh) were electrocopolymerised on graphite electrode for cholesterol biosensor development[58]. One of the most interesting developments of conducting polymer (Poly(4-(2,5-di(thiophene-2-yl)-1H-pyrrole-1-yl)benzamine) (Poly(SNS-NH₂)) electrode modified with multi-walled carbon nanotube could be used for the biosensor for the detection of acetylcholinesterase [59].

2.7. Nanocomposite

Mixing of two or more dissimilar nanomaterials coated on the electrode surface called nanocomposite. It has unique physical, electrical, optical and chemical properties. The major advantages of the composite electrode materials are to enhance the electro active surface and good electrical contact between components and transducers. The electrocatalytic properties of nanostructured composite of chitosan-polypyrrole (CS-PPy) are widely used for the detection of glucose, the reported LOD value is 1.55×10^{-5} M [60]. The advent of platinum embedded polypyrrole nanowire (PPy-Pt) composite has been deposited on glassy carbon electrode, a new dimension of electrochemical application for biosensor (LOD value of 4.5×10^{-7} M) studies [61]. Xue *et al* [62] prepared a ternary gold nanoparticle with polypyrrole and reduced graphene oxide (AuNPs/PPy/RGO) nanocomposite for the direct electron transfer of glucose oxidase and tremendous amperometric response to glucose. The extensive efforts have been developed to improve the sensitive of cholesterol biosensor (6.3 μ M) by using immobilized cholesterol oxidase with horse peroxidase on a poly(thionine) modified glassy carbon (GCE/PTH/ChOx/HRP) composite [63]. The common approach for the immobilization of glucose oxidase on mesoporous carbon and platinum nanoparticle (Pt/OMC)

RF magnetron sputtering. The surface morphology and roughness electrode surface area of ZnO modified electrode exhibits cavities of nano porous film as an effective biosensing area of enzyme by used field emission-scanning electron microscope (FE-SEM) analysis [66]. The environmental scanning electron microscope (ESEM) was used for the analysis of a smooth nature-like structure of carbon nanotubes without aggregation observed on CNTs-chitosan (CNTs-CS) film surface. In this type of smooth like composite provides a biosensing matrix of enzyme based studies due to good biocompatibility, good conductivity and long durability [67]. Ge *et al* [68] have used a linker-free connected graphene oxide/Au nanocluster (GO-Au NCs) composite for biosensor of L-cystein analysis. In this composite, a single layer of GOs was obtained smooth surface and Au NCs showed a uniform surface topography, the measured diameter of about 6 nm.

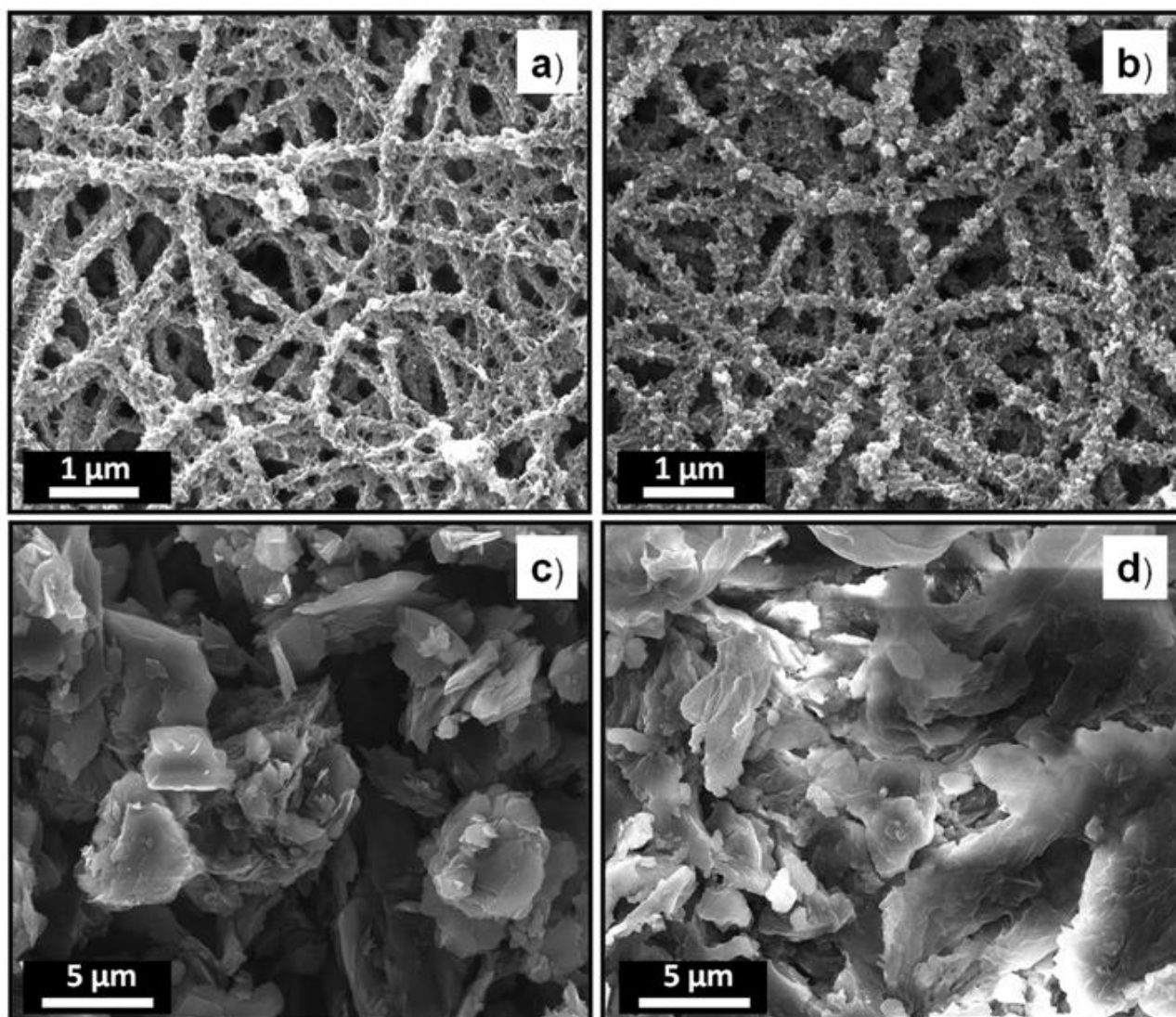


Figure 2. Representative SEM images of (a) nylon 6,6/PBIBA and (b) nylon 6,6/4MWCNT/PBIBA surfaces before GO_x immobilization and (c) nylon 6,6/PBIBA and (d) nylon 6,6/4MWCNT/PBIBA surfaces after GO_x immobilization under optimized conditions. ("Reprinted with permission from (ACS Appl. Mater. Interfaces 6 (2014) 5235-5243). Copyright (2014) American Chemical Society").

Figure.2.shows a layer-by-layer graphene oxide (GO_x) has been synthesized by electro spinning method and it was mixed with MWCNT and Nylon 6,6. In this carbon nanotube composite (Nylon 6,6/MWCNT/PBIBA/ GO_x), which was uniformly wrapped with the nanofiber [69].

4. EFFECT OF pH

All electrocatalytic reactions have been evaluated by acidic to basic (4 to 14) medium, because optimization pH is one of the most important parameter for the study of bio sensing molecules. Electrochemical deposition of gold based laccase electrode used for sensing of enzymatic biosensor analysis. This enzymatic catalyzed reactions are mainly depends on pH and also maintained the maximum peak currents are clearly occur at pH = 5 [70]. Tsopela *et al* [71] studied two different (tungsten/tungsten oxide and platinum/iridium oxide) electrode used for the reduction of O_2 and H_2O_2 . The detection of O_2 and H_2O_2 , Pt/ IrO_2 exhibited more sensitive pH measurement than W/ WO_2 . This type of electrodes were almost demonstrated a linear response wide range of 2.0–12.0. Ascorbic acid is an essential nutrient component for human diet and it can be obtained from fruits. The ascorbic acid biosensors are mainly studied in acidic medium, the optimized pH range between 5.5 and 7.5. The study of as-fabricated poly(3,4-ethylenedioxythiophene)-laurolsarcosinate film biosensor electrode between 5.5 and 8.0 [72]. Zou *et al* [73] have evolved a haemin functionalized graphene oxide electrode for simultaneous determination of ascorbic acid, dopamine and uric acid. The exhibited peak currents of AA, DA and UA at the modified electrode were affected by the pH values of Britton-Robinson buffer solution. The optimized pH oxidation peak currents values of AA, DA and UA were obtained in the range of 3.0 to 8.0. The maximum oxidation peak current values were exhibited at pH = 6. Carbon and silica based electrode modified with niobium oxide, alumina and DNA, exhibited, a potential application in electrochemical biosensor for amitriptyline. The optimized UV-visible results showed a maximum peak current value obtained at pH = 7.5 [74]. The electrochemical response of H_2O_2 at poly(N-isopropylacrylamide)-g-poly(N-isopropylacrylamide-co-styrene) (PNIPAM-g-P(NIPAM-co-St)) with MWCNT (Hb/PNNS/MWCNTs/GCE) composite was examined in 0.1M phosphate buffer solution of pH range from 5.0 to 9.0. [75].

5. ELECTROANALYTICAL TECHNIQUES

5.1. Cyclic voltammetry

CV techniques are widely used a powerful technique for the study of reversible, irreversible and quasi-reversible redox reaction and also it gives useful information regarding mechanism of electrochemical studies. Electrochemically modified electrode of hematoxylin electrode deposited on glassy carbon electrode have been investigated the voltammetric determination of noradrenaline and acetaminophen [76]. The CV data can help to optimize the electrocatalytic processes and the oxidation reaction of noradrenaline. The principle involves the immobilization of acetylcholinesterase on the carbon paste electrode can also be used in biological applications. The voltammetric characterization of biosensor has been characterized by using acetylthiocholine chloride (AsChCl) and the evaluated of

enzyme catalyzed anodic oxidation reaction of thiocholine [77]. Reddy *et al* [78] showed the possibility of electrochemical characterization of p-Nitrophenol by lipase enzyme inhibition method. From this voltmmetry analysis, the anodic peak current increased with an increase of scan rate. The plot of peak current against square root of scan rates, a linear coefficient value of 0.9997. Arya *et al* [79] made a significant contribution in that a polyaniline protected electrode fabricated on gold electrode (PPAuNp/Au) and the modified electrode immobilized with cortisol specific monoclonal antibody (C-Mab). Voltommogram studies have confirmed the PPAuNp/Au composite electrode exhibited repeatable redox behaviour and the LOD of cortisol in the range of 1 pM – 100 nM. In Fig.3.shows the SEM morphological (Skeleton) structure (A,B,C and D) and electrochemical analysis of glucose with chitosan (CS) modified with ferrocene (Fc) and 3D graphene foam (Fc-CS/SWCNT/GOD/3DG) electrode (Fig.3A). Fig.3(B) shows the various concentrations ((a) 0, (b) 10, (c) 15, (d) 20 and (e) 25 nM) of glucose in PBS (0.1 M, pH = 7). The electrode catalyst was displayed the LOD glucose of 1.2 μ M [80].

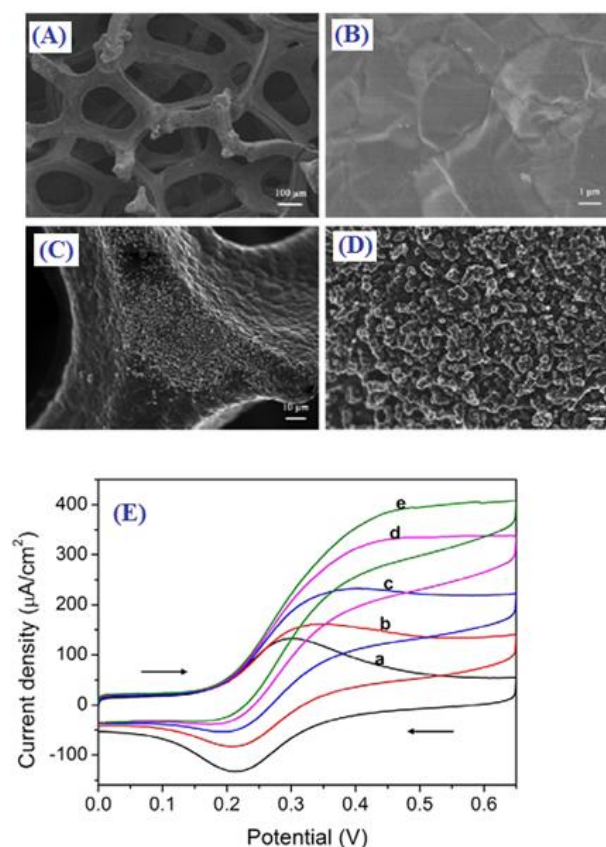


Figure 3. (A and B) SEM images of 3D graphene foam with low and high magnification. (C and D) SEM images of the Fc-CS/SWCNTs/GOD composite film electrodeposited on 3D graphene with low and high magnification. (E) Bioelectrocatalysis of the Fc-CS/SWCNTs/GOD/3DG electrode toward glucose in PBS, the arrows indicated the scan direction of the voltammograms. Glucose concentration was (a) 0, (b) 10, (c) 15, (d) 20, and (e) 25 mM. ("Reprinted with permission from (*ACS Appl. Mater. Interfaces* 6 (2014) 19997-20002). Copyright (2014) American Chemical Society").

5.2. Square wave voltammetry

Square wave voltammetry is one of the sensitive techniques than CV i.e the measurement of accuracy and the limit of detection value up to nano molar (nM) to pico molar (pM). Yadav *et al* [81] reported the detection of chloramphenicol (CAP) using a immobilized poly(4-amino-3-hydroxynaphthalene sulfonic acid) (p-AHNSA) modified with pyrolytic graphite electrode. The square wave voltammetry method was applied for the determination of CAP with a detection limit of 0.02 nM.

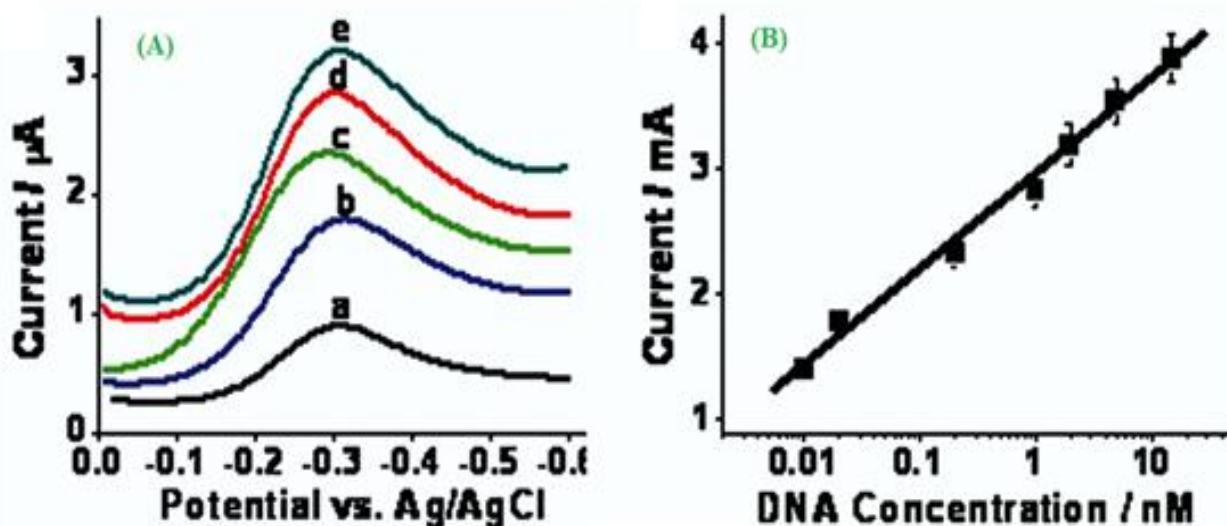


Figure 4. The target DNA concentration shown in the (A) was 0 (a), 0.04 nM (b), 0.2 nM (c), 1 nM (d), and 2 nM (e), separately. (B) Variance of the redox current with the target DNA concentration measured by the E-DNA biosensor with an adjunct probe. ("Reprinted with permission from (*Anal. Chem.* 82 (2010) 9500-9505). Copyright (2010) American Chemical Society").

Figure.4 (A) and (B) illustrated the electrochemical biosensor detection of nucleic acid response exhibited different concentrations using square wave voltammetry at adjunct probe E-DNA. The E-DNA based electrode provide with a limit of detection of 2.0 pM [82]. The use of square wave voltammetry biosensor, the double stranded calf thymus DNA (dsCT-DNA) entrapped polyaniline-polyvinyl sulfonate/indium-tin oxide (PANI-PVS/ITO) composite for chlorpyrifos and malathion [83]. Yola *et al* [84] developed a high sensitive method for the detection (2.0×10^{-15} M) of DNA (5'-TA CCG CGT GCT CGA GCT-(CH₂)₃-SH-3' single-stranded probe) hybridization on modified with Fe@Au nanoparticle involving 2-aminoethanethiol (AET) functionalized graphene oxide electrode. The biosensor of functionalized polypyrrole nanotube arrays modified with a tripeptide (Gly-Gly-His), the electrode allow easily functionalization with α -carboxylic acid. In this case, the electrochemical determination of copper ions (Cu²⁺) has been studied [85].

5.3. Differential pulse voltammetry (DPV)

Several methods have been extensively applied for the development of biosensor applications, like CV, amperometry and square wave voltammetry. Among these methods, DPV exhibit an excellent compatibility, high sensitivity and easily handled. Noaradrenalin (NA) and acetaminophen (AC) are electroactive compound, they can be detected by hematoxylin modified glassy carbon electrode. The electrocatalytic oxidation of NA and AC simultaneous measurement by using DPV [86]. The recent surge of flower-like morphology of zinc oxide (ZnO) nanostructure has been synthesized by hydrothermal method. The DNA immobilizations are mainly focused on interaction of physically immobilized single stranded thiolate DNA (SS th-DNA) and the nanostructure of ZnO. The assembled immobilized electrode can quantify the target molecule of ss th-DNA [87]. Hu *et al* [88] employed a simple and irreversible electrochemical biosensor of glucose by Cv and DPV. Fig.5.shows that the glucose oxidation concentrations increases with increasing of peak current. The development of biosensors glucose oxidation LOD value of 0.015 mM.

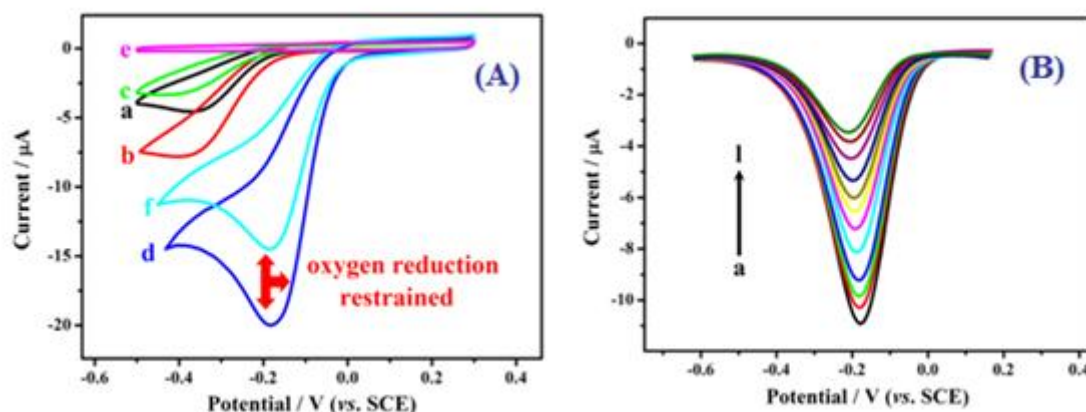


Figure 5. (A) Cyclic voltammograms in air-saturated 0.1 M, pH 7.4 PBS at (a) an electrochemically pre-treated bare Au electrode, (b) after formation of Pt@BSA layer, (c) after cross-linking reaction with GA, after covalent immobilization of GOD in the (d) presence and (e) absence of dissolved oxygen, and (f) with the addition of 6.55 mM glucose to air-saturated buffer. (Scan rate: 50 mV s^{-1}). (B) Differential pulse voltammograms of GOD/GA/Pt@BSA-modified Au electrode in air-saturated 0.1 M, pH 7.4 PBS buffer (under the optimized conditions) with the glucose concentration increased from a to l (0.05, 0.55, 1.55, 3.55, 5.05, 6.05, 6.55, 7.55, 9.55, 11.05, 12.05 mM glucose injection, respectively). ("Reprinted with permission from (ACS Appl. Mater. Interfaces 6 (2014) 4170-4178). Copyright (2014) American Chemical Society").

The electrochemical biosensor of vitamin B₁ on pre-treated multi-walled carbon nanotube paste electrode (PMWCNTPE) modified with ds-DNA has been studied by differential pulse voltammetry [89]. A double strand DNA modified immobilized electrode are extensively used for electrochemical biosensor of morphine. The oxidation event owing to their sensor and real sample analysis were obtained from urine and blood plasma samples [90]. An electrochemical anti-oxidant biosensor based

on electrochemical entrapped dsDNA immobilization on screen-printed electrode has been used for detection of quanine [91].

5.4. Amperometry technique (*i* vs *t* curve)

Amperometry technique has a powerful tool for the determination of biosensor analysis up to low level and it has highly sensitivity, selectivity and simplicity. In a typical amperometric experiment mainly explained by Cottrell equation (Eq. 1)

$$i(t) = nFAC\sqrt{\frac{D}{\pi t}} \quad (\text{Eq.1})$$

The main parameter of *i*-is current and *t*-is time. A novel multi-walled carbon nanotube modified with redox dye Nile Blue (NB) and co-immobilized with horseradish peroxidase (MWCNT/NB/NAF/HRP) composite served as an excellent hot matrices for a second generation of amperometric biosensor.

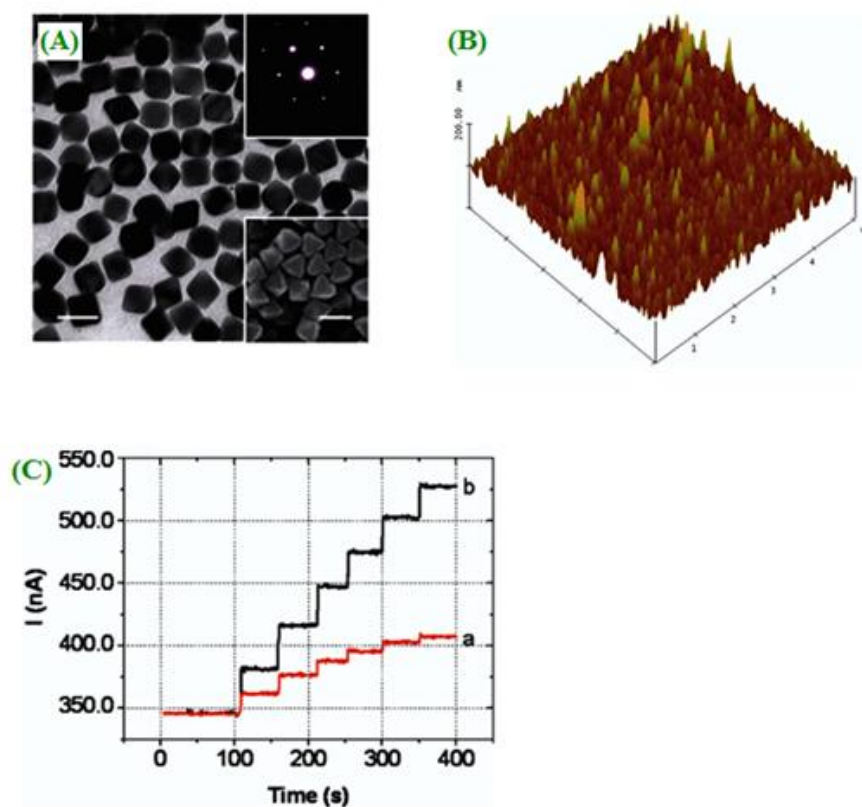


Figure 6. Typical TEM (A) image of gold nanooctahedra. (B) Typical tapping mode AFM height image of GO_x immobilized on a Au nanooctahedra surface. Single-layered Au nanooctahedra with 2.5 μL of 2.5 mg/mL glucose oxidase. (C) Current responses of a single-layered (a) and a five-layered (b) Au nanooctahedra/GO_x system upon successive additions of 0.01M glucose aliquots (50 μL each). ("Reprinted with permission from (*J. Phys. Chem. C* 112 (2008) 3605-3611). Copyright (2008) American Chemical Society").

The impregnated composite were used as an electrode material in electrocatalytic activity for the reduction of hydrogen peroxide [92]. Similarly, the other interesting co-immobilization horseradish and glucose oxidase on silver nano cube with chitosan ($\text{Go}_x\text{-CS-HRP/AgNCs-CS}$) nanocomposite film electrode has been also reported for the oxidation of glucose biosensor applications [93]. Carbonic acid immobilization of a core-shell ceria oxidase-polyaniline ($\text{GCE/CeO}_2\text{-PANI/CA}$) nanocomposite have been shown to exhibit better electrocatalytic activity of carbonic acid in human blood [94]. A third generation of biosensor detection of uric acid by using ferrocene (Fc) induced electro active uricase (UO_x) deposited with nafion on glassy carbon electrode ($\text{Naf/UO}_x\text{/Fc/GCE}$) composite has been also reported [95].

The biosensors for the amperometric detection of glucose response range from 0.125 to 12 mM (Fig.6) and the sensitivity of $0.07 \mu\text{A mM}^{-1}$. Moreover, this type of glucose oxidation has been developed on the parallelogram shape (SEM) and layered structure (AFM) on gold based (Au nanooctahedra/ GO_x) composite [96]. Rahman *et al* [97] have studied poly-5,2':5,2'-tetrathiothiophene-3'-carboxylic acid (poly-TTCA) layer electrode immobilized with hydrazine and horseradish peroxidase (HRP) for the development of amperometric biosensor.

5.5. Electrochemical impedance spectroscopy (EIS)

This technique has been widely used in many electrochemical studies (To monitor the electrode surface properties) and it may apply to investigate the change in charge transfer resistance (R_{CT}) value. Such as electrochemical sensors, corrosion, super capacitors and batteries.

The sulfite oxidase (SO_x) immobilized with nano composite of Prussian blue nanoparticle/polypyrrole film electrodeposited on gold electrode ($\text{SO}_x\text{/PBNPs/PPY/Au}$). The composite electrode has been investigated the R_{CT} value by using EIS analysis. The reported R_{CT} value of 650Ω for PBNPs/PPY/Au composite and 1300Ω for $\text{SO}_x\text{/PBNPs/PPY/Au}$ electrode. In this results are clearly explained the binding of SO_x onto the PBNPs/PPY/Au electrode exhibited poor electrical conduction at low frequency ($<10 \text{ kHz}$) value [98]. The EIS of deoxy ribonucleic acid (DNA) biosensor based multi-walled carbon nanotube deposited on Ag- TiO_2 composite for labile-free phosphinothricin acetyltransferase gene [99]. The nano molar detection of aptamar based thrombin by pyrolyzed carbon film electrode, the electrochemical biosensor exhibited high sensitivity and selectivity of thrombin [100]. The glucose oxidase biosensor has been detected, the limit of detection value of $15.6 \mu\text{M}$ and the sensitivity of $9.66 \times 10^{-7} \Omega^{-1} \text{ mM}^{-1}$ by used immobilized glucose oxidase gold mercaptopropionic acid self-assembled monolayer (Au-MPA- GO_x SAMS) electrode [101]. Recently, ultrasensitive impedometric biosensors of bovinserum albumin (BSA) modified with MWCNT on GCE (BSA/MWCNT/GCE) composite studied for the detection of buprenorphine hydrochloride (BN).

Fig.7.shows the immobilization electrode of DNA modified gold nanoparticle (DNA/AuNPs) at various concentrations and the estimated LOD of 1pM [102].

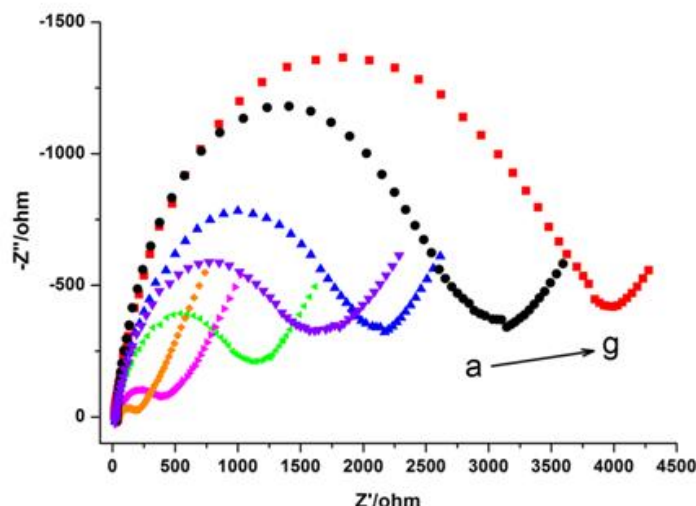


Figure 7. Nyquist plots of impedance spectra obtained by the DNA sensor after incubation with different concentrations of target DNA for 1.5 h and 10 nM GNPs for another 0.5 h: (a) 1 pM; (b) 10 pM; (c) 100 pM; (d) 1 nM; (e) 10 nM; (f) 100 nM; (g) 500 nM. ("Reprinted with permission from *ACS Appl. Mater. Interfaces* 6 (2014) 7579-7584). Copyright (2014) American Chemical Society").

6. ANALYTICAL TECHNIQUE (UV-VISIBLE SPECTROPHOTOMETER)

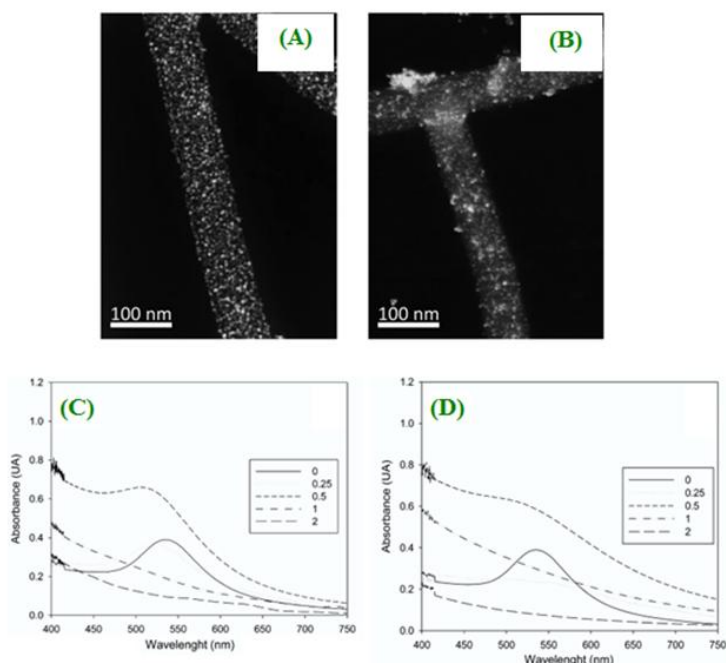


Figure 8. Low-voltage ADF-STEM imaging of nanocomplexes at MPS/AuCl₄⁻ ratios of (A) 0.25, (B) 0.5. UV-visible spectra of nanocomplexes synthesized with the different thiol/AuCl₄⁻ ratios tested in this work. VP₆-Au nanocomplexes without coating are denoted as 0. (a) MPS-coated nanocomplexes. (b) GlcC₅SH-coated nanocomplexes. ("Reprinted with permission from *Langmuir* 30 (2014) 14991-14998). Copyright (2014) American Chemical Society").

The UV-visible spectrum is plotted the graph of absorbance against wavelength, the molecules are commonly exposed to light having possible energy electronic transitions occur to $n \rightarrow \pi^*$ or $\pi \rightarrow \pi^*$. The electrochemical biosensor of DNA/hemin/nafion-graphene/GCE modified electrode have been used to investigate the DNA damage attributed to the benzo(a)pyrene enzyme and also study the feasibility of hemine/H₂O₂ system mimicking the benzo(a)pyrene enzymatic effect by UV-visible spectrophotometer [103]. LaF₃ doped CeO₂ (LaF₃-DP-CeO₂) composite immobilized with myoglobin for the electrochemical determination of nitrite biosensor. By using UV-visible spectrum is an important tool, which gives sufficient structural information on the possible denaturation of heme protein [104]. Zhong *et al* [105] have compared two different electrode materials for glucose amperometric biosensor. By using UV-visible spectrophotometry, PANI absorption peak exhibited at 328 and MWCNT-PANI occur at 630 nm.

This is due to clearly indicated that a strong interaction between PANI and MWCNT-PANI electrode. A typical advantages of ultraviolet visible absorption spectroscopy has been used to detect blue shift (520 and 510 nm) of thiol/AuCl₄⁻ ratio by used a linear ligand of sodium 3-mercapto-1-propane sulfonate (MPS)-coated complex (Fig.8) [106].

7. REAL SAMPLE ANALYSIS

Table 1. Determination of the concentration of BPA of the water samples using the proposed sensor. ("Reprinted with permission from (*ACS Appl. Mater. Interfaces* 7 (2015) 7492-7496). Copyright (2015) American Chemical Society").

Sample	FLD-HPLC (ng/mL) real value \pm SD	Spiked (ng/mL)	Measured (ng/ mL) ^a mean ^a \pm SD ^b	Recovery (%)
Tap water	0.2 \pm 0.1	0.5	0.67 \pm 0.013	96.0
		2	2.15 \pm 0.070	97.5
		5	5.32 \pm 0.23	102.4
River water	1.2 \pm 0.2	0.5	1.71 \pm 0.027	102.0
		2	3.29 \pm 0.15	104.5
		5	6.06 \pm 0.34	97.2

^aThe mean of five experiments. ^bSD = standard deviation.

The DNA based immobilized graphene/cadmium sulphide (DNA/GR-CdS/GCE) electrode, which could apply for the electrochemical biosensor applications. The modified electrode has been

used to determine the content of phenformin obtained from the commercial tablet. DPV and HPLC techniques measured the obtained product of phenformin [107]. The electrochemical DNA nanobiosensor on water sample has been tested with genotoxicity method, Ames test which is the main tool for the analysis of genotoxicity of environmental pollution [108]. Similarly, bioluminescent bacteria has been found in waste water sample by immobilized double stranded calf thymus DNA modified screen printed electrode [109]. A new modified luteolin (Lu) immobilized on functionalized multi-walled carbon nanotube modified glassy carbon (*f* MWCNT/GCE) electrode for real sample analysis, especially Lu was studied in pharmaceutical sample, dairy products and urine sample [110]. High performance liquid chromatography (HPLC) can be used as an analytical technique for the evaluation of real sample (Tap and river water) analysis; the evaluated samples are listed in Table.1 [111].

8. KINETIC STUDIES (MICHAELIS-MENTEN)

Michaelis and Menten have proposed a simple model of reversible reaction of enzyme substrate complex and the complex split into product. The rate of kinetic catalytic reaction K_m has been evaluated by using Lineweaver-Burk equation (Eq.2) [112].

$$\frac{1}{I_{SS}} = \frac{1}{I_{Max}} + \frac{K_{app}^M}{I_{Max}C} \quad (\text{Eq.2})$$

Where I_{SS} steady-state is current after the addition of substrate, C- is concentration of the bulk substrate, I_{Max} is the maximum current and K_{app}^M value obtained from slope and intercept of the plot of reciprocal of the steady-state current. Dong *et al* [113] have used a new porous nanomaterials of zirconium phytate (Zr-IP₆) modified with horse radish peroxide (HRP) and nafion (Nafion/HRP/Zr-IP₆) composite electrode was employed to measure the K_{app}^M value of 0.306 mM. On the other hand, horseradish peroxide (HRP) immobilization on Ag@C core-shell modified with indium-tin oxide (HRP-Ag@C/ITO) electrode exhibited higher bioactivity, greater affinity to H₂O₂ and the calculated biosensor of K_{app}^M value of 3.75 x 10⁻⁵ M [114]. The immobilization of glucose oxidase with chitosan-gold nanoparticle film was prepared via electrodeposition method directly through electrochemical glucose biosensor application and to estimate K_{app}^M value of 3.5 mM [115]. Recently the electrochemical biosensor analysis of lactase dehydrogenase (LDH) immobilized with nano zinc rod and gold (Au/Nano ZnO/LDH) has been studied using amperometry method to evaluate the K_{app}^M value [116].

9. ANALYTICAL PARAMETERS

Nugent *et al* [117] have discussed two important parameters for the study of inhibition as well as reactivation efficiency. The stock solutions of biological (Acetylcholinesterase and methyl parathion) molecules were prepared in phosphate buffer solution. The modified electrode was inhibited

for 5-10 minutes in 5 ml standard solution of MP or AChCl. This kind of inhibited/immobilized electrode, the electrochemical parameter of $I(\%)$ can be calculated from the amperometric biosensor equation (Eq.3).

$$I(\%) = \frac{I_0 - I_1}{I_0} \times 100 \tag{Eq.3}$$

Similarly, the reactive efficiency (R%) has been estimated the following equation (Eq.4)

$$R(\%) = \frac{I_r - I_1}{I_0 - I_1} \times 100 \tag{Eq.4}$$

By using sensor analysis, Δ is change of biosensors peak current recorded in square wave voltammetry method. This is another kind of electrochemical parameter has been identified the calculated by the applied equation (Eq.5).

$$\Delta = \frac{I_0 - I}{I_0} \tag{Eq.5}$$

Where I_0 is the biosensor current before the addition of sensor sample and I is the biosensors peak current after the addition of sensor sample [118]. Chen et al [119] studied graphene oxide-dopamine complex to estimate the k_d (dissociation constant) value form Langmuir adsorption isotherm equation is as follows (Eq.6).

$$\frac{[DA]}{\Delta I} = \frac{[DA]}{\Delta I_{Max}} + \frac{k_d}{\Delta I_{Max}} \tag{Eq.6}$$

In order to maintain fragile dopamine bioactivity during the electrochemical measurement studies.

The comparisons of different electrodes, biomolecules, techniques, lower limit of detection and accuracy values have been discussed in Table. 2. From the over all studies, glucose biosensors exhibited maximum cited literatures have been optimized by amperometric method.

Table 2. Comparison of electroanalytical parameters for various films modified electrode towards different analytes

S.N	Electrodes	Analytes	Methods	LOD	Sensitivity	Ref.
1	GC/CNT/Pt/GOx	Glucose	Amperometry	0.5 μM	2.11 $\mu\text{A mA}^{-1}$	[120]
2	Exfoliated graphene nano plate	Glucose	Amperometry	10 μM	14.17 $\mu\text{AmM}^{-1} \text{cm}^{-2}$	[121]
3	SWCNT/Au/Pd	Glucose	Amperometry	2.3 nM	2.6 $\mu\text{A mM}^{-1} \text{cm}^{-2}$	[122]
4	GOx-Graphene-CS	Glucose	Cyclic voltammetry	0.02 mM	37.93 $\mu\text{A mM}^{-1} \text{cm}^{-2}$	[123]
5	RGO/Nafion	Paraxon	Amperometry	0.137 μM	10.7 $\mu\text{A mM}^{-1}$	[124]
6	Graphene/Pt	Cholesterol	Amperometry	0.2 μM	2.07 $\mu\text{A mM}^{-1} \text{cm}^{-2}$	[125]
7	Graphene/AuNPs/CS	Glucose	Amperometry	180 μM	99.5 $\mu\text{A mM}^{-1} \text{cm}^{-2}$	[126]
8	N doped	Glucose	Amperometry	1.2 μM	149 $\mu\text{A mM}^{-1}$	[127]

	CNT/MWCNT					
9	RGO/PPy/PSS-g-PPy	Hypoxanthane	Amperometry	10 nM	673 $\mu\text{A mM}^{-1} \text{cm}^{-2}$	[128]
10	GOx/C ₆₀ /Fc/CS	Glucose	Chronoamperometry	3 nM	234.67 $\mu\text{A mM}^{-1} \text{cm}^{-2}$	[129]
11	CS-Fc/GO/GOx	Glucose	Amperometry	7.6 μM	10 $\mu\text{A mM}^{-1} \text{cm}^{-2}$	[130]
12	Graphene/CNT/Nafion/AuPtNPs	H ₂ O ₂	SWV	0.17 μM	3.7 x 10 ² $\mu\text{A mM}^{-1}$	[131]
13	Graphene oxide/PB	Glucose	Amperometry	122 nM	408.7 $\mu\text{A mM}^{-1} \text{cm}^{-2}$	[132]
14	Graphene-Fe ₃ O ₄	H ₂ O ₂	Amperometry	0.6 μM	132 $\mu\text{A mM}^{-1} \text{cm}^{-2}$	[133]
15	RGO/PB	Glucose	Amperometry	8.4 μM	59 $\text{mA M}^{-1} \text{cm}^{-2}$	[134]

*GOx– Glucose oxidase; SWCNT-Single walled carbon nanotubes; CS – Chitosan; Ppy – Polypyrrole; Fc – Ferrocene; PB - Prussian blue; RGO – Reduced graphene oxide; PSS-g-PPy – Poly(styrenesulfonic acid g- polypyrrole); C₆₀– Fullerene; SWV- Square wave voltammetry.

10. CONCLUSIONS

Nanostructured electrodes are an important and promising tool for the analysis of electrochemical applications. Especially, in this review we have highlighted to odorize electrode materials and the applied electrochemical technique for application in biosensor field. We found varying reported literatures have been tabularized with different nanostructured electrodes and its bioactive detectivity and sensitivity decorated. The amperometric biosensors of glucose oxidase reaction was one of the most cited article of electrochemical biosensor studies. Most of the authors are mainly focused on cost effective electrode, lowest limit of detection, high sensitivity and long term stability for the evaluation of biosensors applications.

ACKNOWLEDGEMENTS

The research work was supported by the Ministry of Science and Technology, Taiwan and India-Taiwan Science and Technology Cooperation program, DST, India.

References

1. L. Wang, X. Zhang, H. Xiong, S. Wang, *Biosens. Bioelectron.* 26 (2010) 991-995.
2. J. Wang, G. Rivas, X. Cai, E. Palecek, P. Nielsen, H. Shiraishi, N. Dontha, C. Parrdo, M. Chicharro, P.A.M. Farias, F.S. Valera, D.H. Grant, M. Ozsoz, M.N. Flair, *Anal. Chim. Acta* 347 (1997) 1-8.
3. J. Wang, *Anal. Chim. Acta*, 469 (2002) 63-71.
4. B.P. Simon, M. Cortina, M. Campus, C.C. Blanchard, *Sens. Actuators, B* 129 (2008) 459-466.
5. M. Campas, B.P. Siman, J.L. Marty, *Seminars in cell & development biology* 20 (2009) 3-9.
6. E.H. Asl, I. Palchetti, E. Hasheminejed, M. Mascini, *Talanta* 115 (2013) 74-83.
7. S. Prakash, T. Chaterabarty, A.K. Sing, V.K. Shani, *Biosens. Bioelectron.* 41 (2013) 43-53.
8. L. Ding, A.M. Bond, J. Zhai, J. Zhang, *Anal. Chim. Acta* 797 (2013) 1-12.
9. J. Cao, T. Sun, K.T.V. Grattan, *Sens. Actuators, B* 195 (2014) 332-351.

10. R. Ramachandran, V. Mani, S.M. Chen, R. Saraswathi, B.S. Lou, *Int. J. Electrochem. Sci.*, 8 (2013) 11680-11694.
11. S.M. Chen, R. Ramachandran, V. Mani, R. Saraswathi, *Int. J. Electrochem. Sci.*, 9 (2014) 4072-4085.
12. R. Ramachandran, V. Mani, S.M. Chen, G. Gnanakumar, M. Govindasamy, *Int. J. Electrochem. Sci.*, 10 (2015) 859-869.
13. K.J. Babu, A. Zahoor, K.S. Nahm, R. Ramachandran, M.A.J. Rajan, G. Gnanakumar, *J. Nanopart. Res.*, 16 (2014) 2250.
14. J.F. Wu, M.Q. Xu, G.C. Zhao, *Electrochem. Commun.*, 12 (2010) 175-177.
15. M. Zhou, J. Guo, L.P. Guo, J. Bai, *Anal. Chem.*, 80 (2008) 4642-4650.
16. C. Shan, Y. Yang, J. Song, D. Han, A. Ivaska, L. Niu, *Anal. Chem.*, 81 (2009) 2378-2382.
17. L. Wang, X. Zhan, H. Xiong, S. Wang, *Biosens. Bioelectron.* 26 (2010) 991-995.
18. M. Zhou, Y. Zhai, S. Dong, *Anal. Chem.*, 81 (2009) 5603-5613.
19. T. Liu, H. Su, X. Qu, P. Ju, L. Cui, S. Ai, *Sens. Actuators, B* 160 (2011) 1255-1261.
20. Y. Wan, Y. Wang, J. Wu, D. Zhang, *Anal. Chem.*, 83 (2011) 648-653.
21. X. Guo, S. Yang, R. Cui, J. Hao, H. Zhang, J. Dong, B. Sun, *Electrochem. Commun.*, 20 (2012) 44-47.
22. K. Wang, H.N. Li, J. Wu, C. Ju, J.J. Yan, Q. Liu, B. Qui, *Analyst* 136 (2011) 3349-3354.
23. W. Song, D.W. Li, Y.T. Li, Y. Li, Y.T. Long, *Biosens. Bioelectron.* 26 (2011) 3181-3186.
24. W. Sun, Y. Zhang, X. Ju, G. Li, H. Gao, Z. Sun, *Anal. Chim. Acta* 752 (2012) 39-44.
25. F. Xiao, Y. Li, X. Zan, K. Liao, R. Xu, H. Duan, *Adv. Funct. Mater.*, 22 (2012) 2487-2494.
26. C. Guo, H. Sun, X.S. Zhao, *Sens. Actuators, B* 164 (2012) 82-89.
27. H. Ju, H. Sun, H. Chen, *Anal. Chim. Acta* 327 (1996) 125-132.
28. S. Poorahong, S. Santhosh, G.V. Ramirez, T.F. Tseng, J.I. Wang, P. Kanatharana, P. Thavarunkum, J. Wang, *Biosens. Bioelectron.* 26 (2011) 3670-3673.
29. C.J. Yuan, C.L. Wang, T.Y. Wu, K.C. Hwang, W.C. Chao, *Biosens. Bioelectron.* 26 (2011) 2858-2863.
30. Q.N. Schuvaico, S.V. Dzyadevych, A.V.E. Skaya, S.G. Sauvigne, E. Csoregi, R. Cespuglio, A.P. Soldatkin, *Biosens. Bioelectron.* 21 (2005) 87-94.
31. L. Deng, S. Guo, M. Zhou, L. Liu, C. Liu, S. Dong, *Biosens. Bioelectron.* 25 (2010) 2189-2193.
32. N. Sato, H. Okuma, *Sens. Actuators, B* 129 (2008) 188-194.
33. G. Li, Y. Lin, *Anal. Chem.*, 78 (2006) 835-843.
34. S. Lata, B. Batra, P. Kumar, C.S. Pundir, *Analytical biochemistry* 437 (2013) 1-9.
35. I.M. Apetrei, C. Apetrei, *J. Food engineering* 149 (2015) 1-8.
36. M.B. Gholivand, A.R. Jalavand, H.C. Goicoechea, *Int. J. Biol. Macromol.* 69 (2014) 369-381.
37. C. Lanzello, F. Favero, M.L. Antonelli, C. Tortolini, S. Cannistro, E. Coppari, F. Mazzei, *Biosens. Bioelectron.* 55 (2014) 430-437.
38. Q. Sheng, R. Liu, J. Zheng, *Bioelectrochemistry* 94 (2013) 39-46.
39. H. Shiraishi, T. Itoh, H. Hayashi, K. Takagi, M. Sakane, T. Mori, J. Wang, *Bioelectrochemistry* 70 (2007) 481-487.
40. I. Szymanska, H. Radecka, J. Radecki, D.K. Ligaj, *Biosens. Bioelectron.* 16 (2001) 911-915.
41. V. Mani, B. Devadas, S.M. Chen, *Biosens. Bioelectron.* 41 (2013) 309-3015.
42. T.M.B.F. Oliveira, M.F. Barroso, S. Morais, M. Araujo, C. Freire, P.D.L. Neto, A.N. Correia, M.B.P.P. Oliveira, C.D. Mates, *Bioelectrochemistry* 98 (2014) 20-29.
43. H. Liu, C. Duan, X. Su, X. Dong, Z. Huang, W. Shen, Z. Zhu, *Sens. Actuators, B* 203 (2014) 303-310.
44. H.P. Peng, Y. Hu, P. Liu, Y.N. Deng, P. Wang, W. Chen, A.L. Liu, Y.Z. Chen, X.H. Lin, *Sens. Actuators, B* 207 (2015) 269-276.
45. E. Zor, I.H. Patir, H. Bingol, M. Ersoz, *Sens. Actuators, B* 42 (2013) 321-325.
46. B.D. Malhotra, A. Kaushik, *Thin solid film* 578 (2009) 614-620.

47. S.K. Sukla, S.R. Deshpande, S.K. Shukla, A. Tiwari, *Talanta* 99 (2012) 283-287.
48. H. Liu, C. Duan, X. Su, X. Dong, W. Shen, Z. Zhu, *Ceram. Int.* 40 (2014) 9867-9874.
49. S.K. Mahadev, J. Kim *Sens. Actuators, B* 157 (2011) 177-182.
50. X. Chen, J. Zhu, Z. Chen, C. Xu, Y. Wang, C. Yao, *Sens. Actuators, B* 159 (2011) 220-228.
51. T. Jeyapragasam, R. Saraswathi, *Sens. Actuators, B* 191 (2014) 681-687.
52. R.J. Waltman, J. Bargon, *Can. J. Chem.*, 64 (1986) 76.
53. A. Mohammadi, O. Ingnas, I. Lundstrom, *J. Electrochem. Soc.*, 133 (1986) 947.
54. S. Bhadra, D. Khastgin, N.K. Singha, J.H. Lee, *Prog. Polym. Scie* 34 (2009) 783.
55. F.B. Emre, F. Ekiz, A. Bala, S. Emre, S. Timur, L. Toppare, *Sens. Actuators, B* 158 (2011) 117-123.
56. T.C. Gokoglan, S. Soylemez, M. Kesik, S. Toksabay, L. Toppare, *Food Chem.* 172 (2015) 219-224.
57. F.E. Kanik, M. Kolb, S. Timur, M. Bahadir, L. Toppare, *Int. J. Biol. Macromol.* 59 (2013) 111-118.
58. S. Soylemez, F.E. Kanik, A.G. Nurioglu, H. Akpinar, L. Toppere, *Sens. Actuators, B* 182 (2013) 322-329.
59. M. Kesik, F.E. Kanik, J. Turan, M. Kolb, S. Timur, M. Bahadir, L. Toppare, *Sens. Actuators, B* 205 (2014) 39-49.
60. Y. Fang, Y. Ni, G. Zhang, C. Mao, X. Huang, J. Shen, *Bioelectrochemistry* 88 (2012) 1-7.
61. J. Li, X. Lin, *Biosens. Bioelectron.* 22 (2007) 2898-2905.
62. K. Xue, S. Zhou, H. Shi, X. Feng, H. Xin, W. Song, *Sens. Actuators, B* 203 (2014) 412-416.
63. M.M. Rahman, X.B. Li, J. Kim, B.O. Lim, A.J.S. Ahammad, J.J. Lee, *Sens. Actuators, B* 202 (2014) 536-542.
64. X. Jiang, Y. Wu, X. Mao, X. Cui, L. Zhu, *Sens. Actuators, B* 153 (2011) 158-163.
65. X. Wu, Y. Chai, P. Zhang, R. Yuan, *ACS Appl. Mater. Interfaces* 7 (2015) 713-720.
66. S.A. Mozaffari, R. Rahmanian, M. Abedi, H.S. Amoli, *Electrochim. Acta* 146 (2014) 538-547.
67. Y. Liu, X. Qu, H. Guo, H. Chen, B. Liu, S. Dong, *Biosens. Bioelectron.* 21 (2001) 2195-2201.
68. S. Ge, M. Yan, J. Lu, M. Zhang, F. Yu, J. Yu, *Biosens. Bioelectron.* 31 (2012) 49-54.
69. S.D. Uzun, F. Kayaci, T. Uyar, S. Timur, L. Toppare, *ACS Appl. Mater. Interfaces* 6 (2014) 5235-5243.
70. F.W.P. Ribeiro, M.F. Barroso, S. Morais, S. Viswanathan, P.D.L. Neto, A.N. Correia, M.B.P.P. Oliveira, C.D. Matos, *Bioelectrochemistry* 95 (2014) 7-14.
71. A. Tsopela, A. Lale, E. Vanhov, O. Reynes, I. Seguy, *Biosens. Bioelectron.* 61 (2014) 290-297.
72. Y. Wen, J. Xu, M. Liu, D. Li, L. Lu, R. Yue, H. He, *J. Electroanal. Chem.* 674 (2012) 71-82.
73. H.L. Zou, B.L. Li, H.Q. Luo, N.B. Li, *Sens. Actuators, B* 207 (2015) 535-541.
74. J.P. Marco, K.B. Borges, C.R.T. Tarley, E.S. Ribeiro, A.C. Pereira, *J. Electroanal. Chem.* 704 (2013) 159-168.
75. G. Zhang, N. Yang, Y. Ni, J. Shen, W. Zhao, X. Huang, *Sens. Actuators, B* 158 (2011) 130-137.
76. N. Nasirizadeh, H.R. Zare, *Talanta* 80 (2009) 656-663.
77. P. Raghu, T.M. Reddy, K. Reddaiah, B.E.K. Swamy, M. Sreedhar, *Food Chem.* 142 (2014) 188-196.
78. K.G. Reddy, G. Madhavi, B.E.K. Swamy, *J. Mol. Liq.* 198 (2014) 181-186.
79. S.K. Arya, A. Dey, S. Bhansali, *Biosens. Bioelectron.* 28 (2011) 166-173.
80. J. Liu, X. Wang, T. Wang, D. Li, F. Xi, J. Wang, E. Wang, *ACS Appl. Mater. Interfaces* 6 (2014) 19997-20002.
81. S.K. Yadav, B. Agarwal, P. Chandra, R.N. Goyal, *Biosens. Bioelectron.* 55 (2014) 337-342.
82. K. Yang, C.Y. Zhang, *Anal. Chem.* 82 (2010) 9500-9505.
83. N. Prabhakar, G. Sumanna, K. Arora, H. Sing, B.D. Malhotra, *Electrochimica Acta* 53 (2008) 4344-4350.
84. M.L. Yola, T. Eren, N. Atar, *Electrochim. Acta* 125 (2014) 38-47.

85. M. Lin, X. Hu, Z. Ma, L. Chen, *Anal. Chim. Acta* 746 (2012) 63-69.
86. N. Nasirizadeh, H.R. Zare, *Talanta* 80 (2009) 656-663.
87. M. Tak, V. Gupta, M. Tomar, *Biosens. Bioelectron.*59 (2014) 200-207.
88. C. Hu, D.P. Yang, F. Zhu, F. Jiang, S. Shen, J. Zhang, *ACS Appl. Mater. Interfaces* 6 (2014) 4170-4178.
89. P.K. Brahma, R.A. Dar, K.S. Pitre, *Sens. Actuators, B* 177 (2013) 807-812.
90. R.P. Talemi, M.H. Mashhadizah, *Talanta* 131 (2015) 460-466.
91. L.D. Mallo, S. Hernandez, G. Marrazza, M. Mascini, L.T. Kubota, *Biosens. Bioelectron.*21 (2006) 1374-1382.
92. A.K. Upadhyay, Y.Y. Peng, S.M. Chen, *Sens. Actuators, B* 141 (2009) 557-565.
93. P. Yang, L. Wang, Q. Wu, Z. Chen, X. Lin, *Sens. Actuators, B* 194 (2014) 71-78.
94. M. Sing, N. Nesakumar, S. Sethuraman, U.M. Krishnan, J.B.B. Rayappan, *J. Colloid Interface Sci.* 425 (2014) 52-58.
95. T. Ghosh, P. Sarkar, A.P.F. Turner, *Bioelectrochemistry* 102 (2015) 1-9.
96. X.J. Huang, C.C. Li, B. Gu, J.H. Kim, S.O. Cho, Y.K. Choi, *J. Phys. Chem. C* 112 (2008) 3605-3611.
97. M.A. Rahman, M.S. Won, Y.B. Shim, *Biosens. Bioelectron.*21 (2005) 257-265.
98. R. Rawal, C.S. Pandir, *Biochem. Eng. J.* 71 (2013) 30-37.
99. Z. Na, Y. Tao, J. Kui, S.C. Xia, *Chin. J. Anal. Chem.* 38 (2010) 301-306.
100. J.A. Lee, S.H. Wang, J. Kwak, S.I. Park, S.S. Lee, K.C. Lee, *Sens. Actuators, B* 129 (2008) 372-379.
101. R.K. Shervedani, A.H. Mehrjardi, N. Zamiri, *Bioelectrochemistry* 69 (2006) 201-208.
102. Y. Yang, C. Li, L. Yin, M. Liu, Z. Wang, Y. Shu, G. Li, *ACS Appl. Mater. Interfaces* 6 (2014) 7579-7584.
103. Y. Ni, P. Wang, H. Song, X. Lin, S. Kokot, *Anal. Chim. Acta* 821 (2014) 34-40.
104. S. Dong, N. Li, T. Huang, H. Tang, J. Zheng, *Sens. Actuators, B* 173 (2012) 704-709.
105. H. Zhong, R. Yuan, Y. Chai, W. Li, X. Zhong, Y. Zhang, *Talanta* 85 (2011) 104-111.
106. L.C. Fuentes, G.P. Villa, L.A. Palomares, S.E. Moya, O.T. Ramirez, *Langmuir* 30 (2014) 14991-14998.
107. L. Zeng, R. Wang, L. Zhu, J. Zhong, *Colloids and surfaces B: Biointerfaces* 110 (2013) 8-14.
108. H.B. Xu, R.F. Ye, S.Y. Yang, R. Li, X. Yang, *Chin. Chem. Lett.* 25 (2014) 29-34.
109. F. Lucarelli, A. Kicela, I. Palchetti, G. Marrazza, M. Mascini, *Bioelectrochemistry* 58 (2002) 113-118.
110. M. Baghayeri, M. Namadchian, *Electrochim. Acta* 108 (2013) 22-31.
111. Y. Zhou, Y. Cai, L. Xu, L. Zheng, L. Wang, B. Qi, C. Xu, *ACS Appl. Mater. Interfaces* 7 (2015) 7492-7496.
112. R. Kamin, G. Wilson, *Anal. Chem.*, 52 (1980) 1198-1205.
113. J. Dong, Y. Wen, Y. Miao, Z. Xie, Z. Zhang, H. Yang, *Sens. Actuators, B* 150 (2010) 141-147.
114. S. Mao, Y. Long, W. Li, Y. Tu, A. Deng, *Biosens. Bioelectron.*48 (2013) 258-262.
115. Y. Du, X.L. Luo, J.J. Xu, H.Y. Chen, *Bioelectrochemistry* 70 (2007) 342-347.
116. N. Nesakumar, K. Thandavan, S. Sethuraman, U.M. Krishnan, J.B.B. Rayappan, *J. Colloid Interface Sci.* 414 (2014) 90-96.
117. M. Jarczewska, R. Ziolkowski, L. Gorski, E. Malinowska, *Bioelectrochemistry* 96 (2014) 1-6.
118. J.M. Nugent, D. Du, X. Huang, J. Cai, A. Zheng, *Biosens. Bioelectron.*23 (2007) 285-289.
119. J.L. Chen, X.P. Yan, K. Meng, S.F. Wang, *Anal. Chem.*, 83 (2011) 8787-8793.
120. S. Hrapovic, Y. Liu, K.B. Male, J.H.T. Luong, *Anal. Chem.*, 76 (2004) 1083-1088.
121. J. Lu, L.T. Drazal, R.M. Worden, I. Lee, *Chem. Mater.*, 19 (2007) 6240-6246.
122. J.C. Claussen, A.D. Franklin, A.U. Haque, D.M. Portefield, T.S. Fisher, *ACS Nano* 3 (2009) 37-44.
123. X. Kang, J. Wang, H. Wu, I.A. Aksay, J. Liu, Y. Lin, *Biosens. Bioelectron.*25 (2009) 901-905.

124. B.G. Choi, H.S. Park, T.J. Park, M.H. Yang, J.S. Kim, S.Y. Jang, N.S. Heo, S.Y. Lee, J. Kong, W.H. Hong, *ACS Nano* 4 (2010) 2910-2918.
125. R. Sundar, C.R. Raj, *J. Phy. Chem. C* 114 (2010) 21427-21433.
126. S. Shan, H. Yang, D. Han, Q. Zhang, A. Ivaska, L. Niu, *Biosens. Bioelectron.* 25 (2010) 1070-1074.
127. X. Xu, S. Jiang, Z. Hu, S. Liu, *ACS Nano* 4 (2010) 4292-4298.
128. J. Zhang, J. Lei, R. Pan. Y. Xue, H. Ju, *Biosens. Bioelectron.* 26 (2010) 371-376.
129. W. Zhilei, L. Zaijun, S. Xiulan, F. Yinjun, L. Junkang, *Biosens. Bioelectron.* 25 (2010) 1434-1438.
130. J.D. Qiu, J. Huang, R.P. Liang, *Sens. Actuators, B* 160 (2011) 287-294.
131. Q. Zhang, M. Wang, J. Zheng, *Sens. Actuators, B* 160 (2011) 1070-1077.
132. Y. Zheng, X. Sun, L. Zhu, H. Shen, N. Jia, *Electrochim. Acta* 56 (2011) 1239-1245.
133. K. Zhou, Y. Zhu, X. Yang, C. Li, *Electroanalysis* 23 (2011) 862-869.
134. X. Bai, G. Chen, K.K Shiu, *Electrochim. Acta* 89 (2013) 454-460.

© 2015 The Authors. Published by ESG (www.electrochemsci.org). This article is an open access article distributed under the terms and conditions of the Creative Commons Attribution license (<http://creativecommons.org/licenses/by/4.0/>).